3D ELASTIC REGISTRATION IMPROVES HARDI-DERIVED FIBER ALIGNMENT AND AUTOMATED TRACT CLUSTERING

Yan Jin[1], Yonggang Shi[1], Neda Jahanshad[1], Iman Aganj[2], Guillermo Sapiro[2], Arthur W. Toga[1], Paul M. Thompson[1]

[1]Laboratory of Neuro Imaging, Department of Neurology, UCLA School of Medicine, Los Angeles, CA, USA
[2]Deparment of Electrical and Computer Engineering, University of Minnesota, Minneapolis, USA

ABSTRACT

High angular resolution diffusion imaging (HARDI) allows population studies of fiber integrity and connectivity. Tractography can extract individual fibers. For group studies, fibers must be clustered into recognizable bundles found consistently across subjects.

Nonlinear image registration may improve population clustering. To test this, we performed whole-brain tractography with an orientation distribution function based Hough transform method in 20 young adults scanned with 4 Tesla, 105-gradient HARDI. We warped all extracted fibers to a geometrically-centered template using a 3D elastic registration driven by fractional anisotropy maps, to align embedded tracts. Fiber alignment was evaluated by calculating distances among corresponding fibers across subjects. Before and after warping, we performed spectral clustering of the fibers using a *k*-means method, based on eigenvectors of a fiber similarity matrix. In tests with an overlap metric, non-rigid fiber warping yielded more robust clustering results. Non-rigid warping is therefore advantageous for population studies using multi-subject tract clustering.

Index Terms— HARDI, Tractography, Spectral Clustering, Image Registration, Non-rigid Fiber Warping

1. INTRODUCTION

Diffusion tensor MR imaging (DT-MRI [1]) is increasingly used to study pathology and connectivity of white matter pathways in the living brain. Recently, *q*-space diffusion imaging methods have led to even more sophisticated models of the local diffusion propagator. These include high angular resolution diffusion imaging (HARDI [2]), hybrid diffusion imaging (HYDI [3]), and diffusion spectrum imaging (DSI [4]). These more complex diffusion models allow more accurate fiber tractography – correctly reconstructing fibers that mix and cross - and more sophisticated definitions of local diffusion anisotropy [5]. Even so, a major challenge is how to group fibers across subjects in a convenient way for population studies, without prohibitive levels of manual interaction to segment specific tracts in an entire population of scans. Here we assess whether nonlinear registration of images can facilitate the automatic clustering of HARDI-derived fiber sets for large-scale statistical studies.

Many widely available tractography algorithms extract fiber tracts from DTI or HARDI for better visualization of white matter bundles. These include deterministic streamline methods, which follow the principal eigenvector of the diffusion tensor from one voxel to the next [6], and more recent probabilistic techniques [7]. In this study, to obtain sets of fibers for clustering, we use our recent tractography algorithm based on the Hough transform. This method uses a voting procedure to perform an exhaustive search of all candidate fibers based on path integrals in the orientation distribution function (ODF) field, and their fractional anisotropy (FA) [8]. Once trajectories are extracted, we organize the curves into coherent bundles, by automated fiber clustering.

A typical framework for fiber clustering is first to define a similarity metric (commonly based on distance) and a similarity matrix between all pairs of fibers. The eigenvectors of this similarity matrix are calculated. Finally, a clustering algorithm - for example, *k*-means - classifies the fibers in the spectral space spanned by the first *k* eigenvectors (*k* is the cluster number, usually defined manually). Some classic clustering work has been presented by O'Donnell *et al.* [9] and Wassermann *et al.* [10]. More recently, Bayesian frameworks that take advantage of atlas-based information as priors have been implemented to improve clustering accuracy. There is great interest in improving agreement between automatically extracted clusters and standard neuroanatomical tract definitions [11].

It is highly desirable to cluster fiber tracts into groups consistently in a large population study. An open question, which we address here, is whether this clustering is more successful when fibers have already been pre-aligned across subjects, via deformable image registration. For all of the clustering methods mentioned above, diffusion-weighted images are usually only linearly registered across subjects [9][12]. Surprisingly, non-rigid registration is rarely used before clustering. Here we use a variety of distance and overlap metrics to test whether non-rigid (3D elastic) registration of HARDI data can improve the alignment of embedded tracts. We also assess, in turn, whether the improved fiber alignment may facilitate clustering. The

overall goal of this work is to improve the power of multi-subject analysis of diffusion imaging data, and improve the automation of large-scale tract-based studies.

2. METHODS

2.1. Subjects and image acquisition

HARDI images were acquired as part of a larger study of 374 young adults with a 4 Tesla Bruker Medspec MRI scanner. T1-weighted images were acquired with an inversion recovery gradient echo sequence with parameters: T1/TR/TE=700/1500/3.35 ms, flip angle=8°, slice thickness=0.9mm, and a 256x256x256 acquisition matrix. HARDI images were acquired by single-shot echo planar imaging (EPI) with parameters: TR/TE=6090/91.7ms, 23cm FOV, and a 128x128x55 acquisition matrix. Axial slice thickness =1.79mmx1.79mmx2mm. 105 volumes of images were acquired for each subject: 11 with no diffusion sensitization, that is, T_2-weighted b_0 images and 94 diffusion-weighted images (b = 1159 s/mm^2). As they were recruited for a large genetic study, the subjects were 120 young adult monozygotic twins, 90 same-sex dizygotic twins, and 164 mixed-sex dizygotic twins. The genetic aspects were not pursued in this paper, so the subjects were just treated as individuals. All subjects were right-handed and had no history of head injury or mental illness.

2.2. Registration

Image registration was conducted in four steps [13]:

Step I: Each subject's anatomical T1-weighted image and set of HARDI images were linearly aligned to the Colin27 high-resolution single-subject template [14].

Step II: After eddy current correction with FSL software (http://fsl.fmrib.ox.ac.uk/fsl/), the voxel-wise average of each subject's 11 *b0* images was elastically registered to the same subject's aligned T1-weighted images using inverse-consistent elastic registration [15]. This step used mutual information as a cost function for an elastic deformation model implemented using the spectral method (Fast Fourier Transform). To correct for EPI-related distortions, the resulting 3D deformation fields (which had a 32x32x32 resolution in the frequency domain) for each subject were applied to the rest of the 94 HARDI images. Following EPI distortion correction, FA was computed from the 105-gradient HARDI images using FSL (see later for ODF reconstruction). The rest of the registration steps used distortion-corrected FA images.

Step III: We created a geometrically-centered, minimal deformation target (MDT) from a randomly selected set of 32 subjects' FA maps using a nonlinear viscous fluid registration [16], which allows large deformations without causing singularities in the deformation field (i.e., regions of non-positive Jacobian determinant). All the FA images of each subject were then registered to the MDT by elastic registration [15]. The resulting finer-scale 64x64x64 resolution deformation fields were used to align all subjects' FA images into the same coordinate space.

Step IV: Finally, to better align white matter regions of interest, the MDT and each subject's FA images were thresholded to include only the regions where FA>0.25. Individual thresholded FA images were once again registered to the thresholded MDT, using a third set of 3D 64x64x64 resolution deformation fields. We found in our prior work [13] that this iterative registration process leads to good alignment of FA maps for statistical studies.

2.3. Tractography

We then performed whole-brain tractography with a global probabilistic approach that uses the Hough transform as a voting procedure [8]. We first generated a large number of initial seed points inside the brain. From each initial point, as many passing curves as possible were considered (this could depend on the data resolution and available computational resources). A score was assigned to each curve based on the normalized and dimensionless ODF estimator in q-ball imaging [17], and also considering the FA along the path. Curves with the highest scores were picked as the fibers that passed through each seed point. We extracted fibers for each subject from the linearly aligned HARDI images (after step I in **Section 2.2**) and saved the coordinate points of each fiber in a text document, as a look-up table for later nonlinear alignments.

2.4. Automated fiber clustering

We used the spectral clustering method described in [18]. A similarity matrix (the fiber similarity) was constructed based on the distances between fibers. We used the metric in [9] to calculate the distance between fibers i and j. First, we found the closest point on fiber j for each point on fiber i and stored the distance. The distance was averaged after computing distances from all the points on fiber i. We denote it as d_{ij}. Spectral clustering requires a symmetric matrix. Therefore, we took the average of the directed distances d_{ij} and d_{ji}. As a result, the distance between two fibers became undirected. Then, a Gaussian kernel was applied to convert the distance to a similarity measure A_{ij}= $\exp(-d_{ij}^2/\sigma^2)$. σ determines the range of distances over which fibers may be considered similar. We chose σ =5 voxels, for this study.

An astronomical number of fibers are available when performing multi-subject clustering. To shorten the computation time, we defined a neighborhood (e.g., 5 voxels) around the coordinate points along a fiber. We only calculated the distances between the fibers that crossed this neighborhood of the specified fiber. Other fibers were classified as having no connection with this particular fiber. Next, a normalized graph Laplacian matrix was created, defined as $L = I - D^{-1/2}AD^{1/2}$, where I is the identity matrix

and D is a diagonal matrix, whose diagonal elements are the sum of each row of A_{ij}. By manually setting the cluster number k, the first k generalized eigenvectors of $Lu=\lambda Du$ were computed.

Finally, the k-means algorithm was used to cluster the points (which represent individual fibers) in the space spanned by the k eigenvectors. **Figure 1** shows an example clustering result when k=10 by running the algorithm as described above.

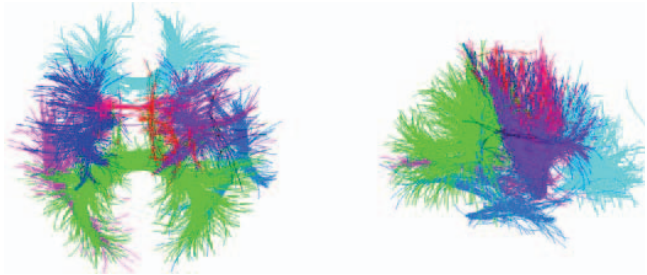

Figure 1. A representative result of spectral clustering in 4-Tesla 105-gradient HARDI data from one individual subject (with k=10 clusters). Each cluster is labeled with a separate color. Top and side views of the brain are shown. Several major tracts are evident, including the *forceps major,* which runs through the splenium of the back of the corpus callosum (*green*), and the fibers running in the callosal *genu* (*light blue*).

2.5. Non-rigid fiber warping

Before performing multi-subject clustering, we also warped the fibers from all subjects by applying the deformation fields generated in **Section 2.2**. We applied all deformation mappings in sequence through tri-linear interpolation. An illustration is shown in **Figure 2**.

2.6. Evaluation

Two metrics were selected to evaluate the performance of non-rigid image registration on fiber alignment. We used the mean distance between the "corresponding" fibers of the two subjects and the percentage of the fibers that had a "better match" after warping. The "corresponding" fibers refer to the two individual fibers in each of two different subjects with the shortest distance between each other. The fiber distance is defined as the mean of the distances from the coordinate points over one curve to the nearest points on the other curve. It is symmetrized by taking the average of two directed distances between the two curves. This is detailed in **Section 2.4**. These corresponding fibers do not necessarily form part of an overall one-to-one mapping of all the fibers between the two subjects. We calculated the mean distance of all the corresponding fibers within these two subjects and used it as an index of registration quality. A "better match" means that a closer corresponding fiber from the other subject is found for a particular fiber in one subject.

To evaluate how fiber warping affected the population clustering, we calculated overlap percentages for the fibers within the same clustered bundle (e.g., the *forceps major* which runs through the posterior region of the corpus callosum) using different neighborhood sizes for the group clustering. The overlap percentage is defined as 100 times the following fraction

$$\frac{\text{fibers clustered to a specific bundle with nbhd } i \cap \text{ with nbhd } j}{\text{fibers clustered to a specific bundle with nbhd } i \cup \text{ with nbhd } j}$$

where nbhd i and j are the neighborhoods (e.g., 5-voxel neighborhoods) used to compute the similarity matrix in **Section 2.4**. Presumably, different neighborhood sizes will produce different clustering results. The overlap percentages before and after warping were compared (see **Results**) to assess how stable the population clustering results were after fiber warping.

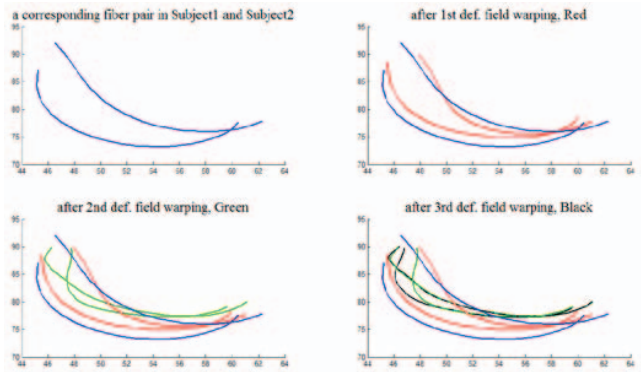

Figure 2. Two "corresponding" fibers are shown (*blue colors, top left;* "corresponding" is defined in **Section 2.6**). These are then warped, step by step, through the three deformation fields generated in the registration step.

3. RESULTS

To make computations easier, two groups, with a total of 20 subjects were selected from the HARDI database of 374 subjects to perform a sample population clustering analysis. Ten subjects were randomly selected and the other ten were those whose deformation fields in the registration step had the greatest magnitude on average across the brain. There were no twin pairs within either group to avoid any genetic influence (artificial resemblance) in the warping results.

3.1. Fiber alignment

In **Table 1**, quantitatively, we show that fiber alignment is indeed improved after using the information from 3D elastic image registration. For each subject, we first calculated the average distances between "corresponding" fibers (defined in **Section 2.6**) with every other subject in the population of each group, and then took the mean of these average distances within a group as group mean distance (G.M.D.). We calculated it both before and after warping. We also counted the percentages of "better matched" (also defined in **Section 2.6**) fibers after warping between that subject and every other subject. Next, a group mean of these

Table 1
Mean fiber matching distances and the percentages of better matched fibers (after versus before warping) from one particular subject to the rest of the sample population.

Group	G.M.D.[1] between corresponding fibers (voxel)			Improved Pct. of G.M.D.	Group Mean B.M.F.[2] Pct.
	Pre-warp	Post-warp	*p*-value of *t* test		
Randomly Selected Subjects	2.44	2.05	2.14×10^{-8}	16%	70%
Most Highly Deviating Subjects	2.89	2.27	2.27×10^{-7}	21%	73%

[1] G.M.D. = Group Mean Distance
[2] B.M.F. = Better Matched Fibers

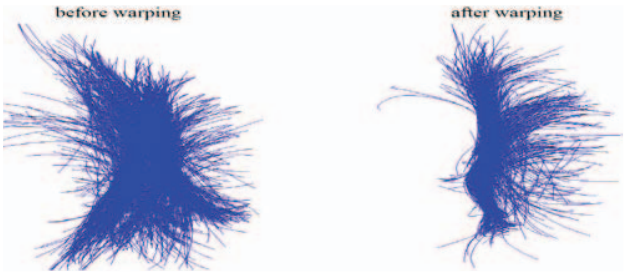

Figure 3. The same fibers of all 10 subjects in the most anatomically deviating group in one cluster are shown, before (*left*) and after (*right*) 3D elastic warping.

percentages was taken as the mean better matched fiber (B.M.F.) percentage for that group. As a result, the G.M.D. between corresponding fibers from one subject to the others was shortened from 2.44 voxels to 2.05 voxels, giving a *p*-value of 2.14×10^{-8} in a paired *t*-test. These statistics were derived for the randomly selected group – a significant 16% improvement. We also analyzed results for the subjects with the greatest anatomical deviation from the mean template, as computed from the deformation maps. For this "most highly deviating" group the G.M.D. dropped from 2.89 voxels to 2.27 voxels with a *p*-value 2.27×10^{-7}, according to a paired *t*-test. Interestingly, a *p*-value 9.95×10^{-4} in a separate *t*-test between the improvements in the two groups indicated that elastic fiber warping was more helpful for the set of subjects whose images deviated more. This is in line with common sense: the method is genuinely better aligning tracts in those with greater initial deviations. On average, the majority of fibers were better aligned (i.e., found a -B.M.F. in another subject) after non-rigid warping in both the randomly selected subgroup (by 70%) and the "most highly deviating" group (by 73%).

To visualize these effects, **Figure 3** shows the same fibers for all ten subjects in the most anatomically deviating group in a particular cluster before and after elastic warping. Clearly, the overall path of the fiber set is "tidier", after warping, and more obviously clustered.

3.2. Clustering robustness

The overlap percentages (defined in **Section 2.6**) for the fibers belonging to the *forceps major* - which travels through the posterior region of the corpus callosum - were calculated for different neighborhood sizes. The neighborhood size is a free parameter needed to compute the similarity matrix for clustering. Taking the 2.5-voxel neighborhood as a reference, we compared it to other neighborhood sizes, by assessing the overlap percentages for each subject from the population clustering results. The mean across the group and the *p*-values of the paired *t*-tests assessing improvements due to warping are shown in **Table 2**. For both groups, we saw significant improvements based on the *p*-values. Therefore, fiber warping does generate more robust results, even when different parameters are used in the clustering algorithm.

Figure 4 shows the *forceps major* bundle in the posterior region of corpus callosum in a representative subject, before and after elastic fiber warping.

Table 2
The mean overlap percentages of fibers in the *forceps major* in the posterior region of the corpus callosum, when different neighborhoods were used to compute the similarity matrix used for clustering (the 2.5-voxel neighborhood was considered as the reference).

Group	Mean Overlap Percentage			
	5 vs. 2.5-voxel neighborhood		8 vs. 2.5-voxel neighborhood	
	Pre-warp	Post-warp	Pre-warp	Post-warp
Randomly Selected Subjects	58%	68%	51%	62%
p-value of *t* test	1.18×10^{-6}		9.59×10^{-9}	
Most Highly Deviating Subjects	93%	96%	69%	95%
p-value of *t* test	0.026		2.67×10^{-6}	

4. DISCUSSION AND FUTURE WORK

In this preliminary work, we showed that the information obtained from nonlinear registration of HARDI may be used to improve fiber alignment for clustering in multi-subject studies. Improved fiber alignment can lead to more robust clustering, even under reasonable variations in the algorithm parameters.

The spatial resolution of the deformation fields in this work was lower than the image resolution, which made interpolation necessary to calculate the fiber positions after warping. In future, we will assess whether fiber alignment would be further improved by running the elastic registration on a finer computational grid. This would avoid

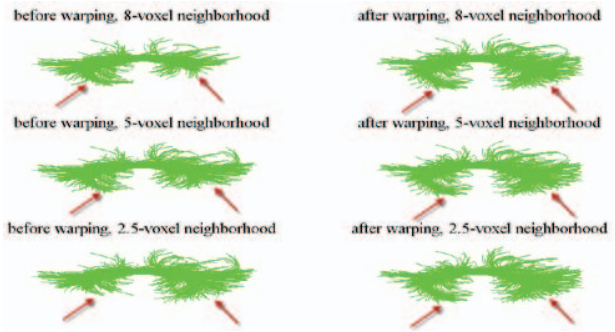

Figure 4. Top views of fibers clustered as the *forceps major* at the back of corpus callosum, using different neighborhood sizes in the spectral clustering method. Arrows point to the regions with different levels of consistency in clustering results with and without fiber warping.

interpolation, and may align features more precisely. The spatial regularity of the applied deformation field is also relevant, and higher-dimensional registrations are not necessarily better. With higher frequency warping, a fiber may become increasingly twisted. This may eventually adversely affect the curvature and smoothness of the original fiber. In the future, we will investigate whether higher-dimensional deformations, with higher spatial frequencies, would further improve fiber alignment, or whether there is an optimal intermediate trade-off.

In this work, we only took advantage of information obtained by registering scalars derived from the diffusion tensor images, which typically have lower resolution than T1-weighted images. Naturally, registration based on a combination of both HARDI and T1-weighted images may further improve fiber alignment [19]. Nevertheless, based on our work, non-rigid fiber warping seems to be a beneficial step before performing clustering in population studies.

5. ACKNOWLEDGMENTS

This work was supported by National Institutes of Health grants R01 EB008432, R01 EB007813, R01 HD050735 and the National Health and Medical Research Council, Australia, grant NHMRC 496682. Additional support was provided by grants R01 EB008281 and P41 RR013642.

6. REFERENCES

[1] P.J. Basser, J. Mattiello, and D. LeBihan, "MR diffusion tensor spectroscopy and imaging," *Biophysical Journal*, 66, pp. 259-67, 1994.

[2] D.S. Tuch, "Q-Ball Imaging," *Magnetic Resonance in Medicine*, 52, pp. 1358-72, 2004.

[3] Y.C. Wu, A.S. Field, and A.L. Alexander, "Computation of diffusion function measures in *q*-space using magnetic resonance hybrid diffusion imaging," *IEEE Transactions on Medical Imaging*, 27, pp. 858–65, 2008.

[4] V.J. Wedeen, P. Hagmann, W.I. Tseng, T.G. Reese, and R.M. Weisskoff, "Mapping complex tissue architecture with diffusion spectrum magnetic resonance imaging," *Magnetic Resonance in Medicine*, 54, pp. 1377–86, 2005.

[5] A.D. Leow, S. Zhu, L. Zhan, K. McMahon, G.I. de Zubicaray, M. Meredith, M.J. Wright, A.W. Toga, and P.M. Thompson, "The tensor distribution function," *Magnetic Resonance in Medicine*, 61, pp. 205-14, 2009.

[6] S. Mori, B.J. Crain, V.P. Chacko, and P.C.M. Van Zijl, "Three dimensional tracking of axonal projections in the brain by magnetic resonance imaging," *Annals of Neurology*, 45(2), pp. 265–69, 1999.

[7] M. Descoteaux, R. Deriche, T.R. Knösche, and A. Anwander, "Deterministic and probabilistic tractography based on complex fibre orientation distributions," *IEEE Transactions on Medical Imaging*, 28, pp.269–86, 2009.

[8] I. Aganj, C. Lenglet, N. Jahanshad, E. Yacoub, N. Harel, P.M. Thompson, and G. Sapiro, "A Hough transform global probabilistic approach to multiple-subject diffusion MRI tractography," *Medical Image Analysis*, in press, 2011.

[9] L.J. O'Donnell and C.F. Westin, "Automatic tractography segmentation using a high-dimensional white matter atlas," *IEEE Transactions on Medical Imaging*, 26, pp.1562-75, 2007.

[10] D. Wassermann, M. Descoteaux, and R. Deriche, "Diffusion maps clustering for magnetic resonance Q-ball imaging segmentation," *International Journal of Biomedical Imaging*, 2008 (526906).

[11] D. Wassermann, L. Bloy, E. Kanterakis, R. Verma, and R. Deriche, "Unsupervised white matter fiber clustering and tract probability map generation: Application of a Gaussian process framework for white matter fibers," *NeuroImage*, 51, pp. 228-41, 2010.

[12] U. Ziyan, M.R. Sabuncu. W.E.L. Grimson, C.F. Westin, "Consistency clustering: a robust algorithm for group-wise registration, segmentation and automatic atlas construction in diffusion MRI," *International Journal of Computer Vision*, 85, pp. 279-90, 2009.

[13] N. Jahanshad, A.D. Lee, M. Barysheva, K.L. McMahon, G.I. de Zubicaray, N.G. Martin, M.J. Wright, A.W. Toga, and P.M. Thompson, "Genetic influences on brain asymmetry: A DTI study of 374 twins and siblings," *NeuroImage*, 52, pp. 455-69, 2010.

[14] C.J. Holmes, R. Hoge, L. Collins, R. Woods, A.W. Toga, and A.C. Evans, "Enhancement of MR images using registration for signal averaging," *Journal of Computer Assisted Tomography*, 22(2), pp. 324-33, 1998.

[15] A.D. Leow, I. Yanovsky, M.C. Chiang, A.D. Lee, A.D. Klunder, A. Lu, J.T. Becker, S.W. Davis, A.W. Toga, and P.M. Thompson, "Statistical properties of Jacobian maps and the realization of unbiased large-deformation nonlinear image registration," *IEEE Transactions on Medical Imaging*, 26, pp. 822-32, 2007.

[16] N. Leporé, Y.Y. Chou, O.L. Lopez, H.J. Aizenstein, J.T. Becker, A.W. Toga, and P.M. Thompson, "Fast 3D fluid registration of brain magnetic resonance images," *Proceedings of SPIE - Medical Imaging*, Vol. 6916, 2008.

[17] I. Aganj, C. Lenglet, G. Sapiro, E. Yacoub, K. Ugurbil, and N. Harel, "Reconstruction of the orientation distribution function in single and multiple shell *q*-ball imaging within constant solid angle," *Magnetic Resonance in Medicine*, 64, pp.554–66, 2010.

[18] U. von Luxburg, "A tutorial on spectral clustering," *Statistics and Computing*, 17(4), pp. 395-416, 2007.

[19] C. Studholme, "Incorporating DTI data as a constraint in deformation tensor morphometry between T1 MR Images," *Information Processing in Medical Imaging, Lecture Notes in Computer Science,* Vol. 4584, pp.223-32, 2007.